Taylor & Francis
Taylor & Francis Group

Canadian Metallurgical Quarterly

The Canadian Journal of Metallurgy and Materials Science

ISSN: 0008-4433 (Print) 1879-1395 (Online) Journal homepage: http://www.tandfonline.com/loi/ycmq20

Factors Affecting the Notch Toughness Properties of High Strength HY80 Weldments

J. T. McGrath, J. A. Gianetto, R. F. Orr & M. W. Letts

To cite this article: J. T. McGrath, J. A. Gianetto, R. F. Orr & M. W. Letts (1986) Factors Affecting the Notch Toughness Properties of High Strength HY80 Weldments, Canadian Metallurgical Quarterly, 25:4, 349-356, DOI: 10.1179/cmq.1986.25.4.349

To link to this article: http://dx.doi.org/10.1179/cmq.1986.25.4.349

Canadian Metallurgical Quarterly, Vol. 25, No. 4, pp. 349–356, 1986.
Printed in Great Britain.

0008–4433/87 $3.00+.00
Canadian Institute of Mining and Metallurgy
Pergamon Journals Ltd.

FACTORS AFFECTING THE NOTCH TOUGHNESS PROPERTIES OF HIGH STRENGTH HY80 WELDMENTS

J. T. McGRATH, J. A. GIANETTO, R. F. ORR and M. W. LETTS
P.M.R.L., Canmet, 568 Booth Street, Ottawa K19 0G1, Canada

(*Received* 31 *July* 1986; *in revised form* 30 *October* 1986)

Abstract—The microstructure/notch toughness property relationship were evaluated for the weld metal and heat affected zone (HAZ) regions in a series of high strength HY80 weldments.

The weld metal notch toughness exceeded targeted Charpy energy levels in HY80 welds deposited by the SAW process using commercially available welding consumables. The superior toughness was associated with a microstructure containing acicular ferrite and a low inclusion content ($0 + S \approx 0.04\%$).

Low toughness in the CGHAZ of real welds and Gleeble simulated specimens resulted from grain boundary embrittlement related to the liquation of sulfide inclusions during welding.

1. INTRODUCTION

The application of the high strength HY steels is limited by the attainment of adequate strength and notch toughness properties in the weld metal and heat-affected zone regions [1]. The problem of optimizing the weld metal strength and toughness is concerned with increasing the proportion of acicular ferrite combined with a low inclusion content [2]. In the case of the coarse grain heat-affected zone (CGHAZ) the quenched and tempered martensitic structure of the base metal has been eliminated by the thermal effects of welding. The resultant CGHAZ will contain a high proportion of untempered martensite combined with grain boundary embrittling effects [3–5]. A further complication arises in evaluating the notch toughness in the CGHAZ in standard butt welds with a single or double vee weld preparation. The through-thickness Charpy notch will sample portions of the weld metal, CGHAZ and base metal. If the CGHAZ is considered as a region of metallurgical heterogeneity in the test section, then the overall notch toughness will be affected [6–8].

The present study was undertaken to quantify the factors which control the notch toughness properties in the weld metal and CGHAZ regions of a series of HY80 weldments deposited by the submerged arc welding process. The targeted notch toughness properties for the HY80 weldments were obtained from consideration of present military standards for submarine fabrication [9]. Although the military standard requires 27 J at −50°C and 81 J at −18°C, it is generally felt that a higher Charpy impact energy should be specified, i.e. 47 J at −50°C and 81 J at −18°C. The latter levels of toughness were taken as target values for both weld metal and heat-affected zone Charpy toughness tests.

2. EXPERIMENTAL

2.1. *Materials and welding procedure*

Studies of heat-affected zone and weld metal microstructure and mechanical properties were made in butt welds deposited in 25 mm thick HY80 high-strength steel. Two heats of HY80 steel are listed in Table 1. All welds were made with heat HT 1 base metal. In the HAZ simulation experiments described in 2.2, heats HT 1 and HT 2 were employed.

The butt welds were made using a single electrode submerged arc welding technique. Welding procedures were developed to provide heat inputs of 1.4–4 kJ/mm for two wire/flux consumable combinations listed in Table 2. All welding was performed using a 2.4 mm dia. electrode with the exception of weld W1 which was made with a 1.6 mm dia. electrode.

The joint designs were modified to accommodate the increased heat input and are shown in Fig. 1 along with the pass sequences to complete each weld. Backgouging, by the carbon arc process, was employed in all procedures prior to deposition of the final passes. The welding parameters selected for the welds are shown in Table 2.

2.2. *Simulation of the HAZ*

The Gleeble 1500 thermal/mechanical simulator was employed to simulate the coarse grain heat-affected zone in the HY80 steel. A peak temperature of 1350°C and cooling times of 11.5 and 45 s represented the cooling rates for welding of a 25 mm plate at 2 and 4 kJ/mm respectively. Heats HT 1 and HT 2 were used in the simulation studies.

The Gleeble specimens, 10 mm × 10 mm × 75 mm were machined from the base materials with the long axis transverse to the plate rolling direction. The simulated CGHAZ was contained in approximately 5 mm of the central portion of the specimen. Following the weld thermal cycling, specimens were notched through-thickness for Charpy-V notch toughness testing.

Mechanical testing

The tensile properties of the welds were assessed from all weld metal tensile specimens. The notch toughness properties of the weld metals were measured from Charpy specimens located 2 mm below the original plate surface on the back-gouged side of the weldments. The weld metal specimens were notched through-thickness at the weld centerline. The HAZ notch toughness of the welds was measured in specimens

Table 1. Chemical composition of HY80 base materials

Base material	Wt%										Hardness
	C	Mn	Si	P	S	Ni	Cr	Mo	Cu	V	DPH
HY80 HT1	0.17	0.30	0.19	0.007	0.014	2.59	1.53	0.42	0.03	0.01	217
HY80 HT2	0.14	0.25	0.21	0.007	0.011	2.59	1.52	0.45	0.04	0.01	299

Heat treatment: HT1—904°C, 70 min, WQ, temper. 715°C, 70 min.
HT2—904°C, 70 min, WQ, temper. 699°C, 70 min.

Table 2. Welding consumables and parameters for submerged arc weld

Series	Wire/flux combinations	Weld No.	Heat input (kJ/mm)	Current DCEP (A)	Wire feed speed (mm/s)	Voltage (V)	Travel speed (mm/s)	Electrical stickout (mm)
A	Linde 95/Oerlikon OP121TT	W1	1.4	325	N/A	30	7.0	13
		W2	2	450	55.0	35	7.8	25
		W3	3	500	62.2	35	5.9	25
		W4	4	600	72.0	35	5.1	25
B	Lincoln LA100/Lincoln 880M	W5	2	450	55.0	35	7.8	25
		W6	3	500	62.2	35	5.9	25
		W7	4	600	76.2	35	5.1	25

Preheat temperature 93°C; interpass temperature 149°C.

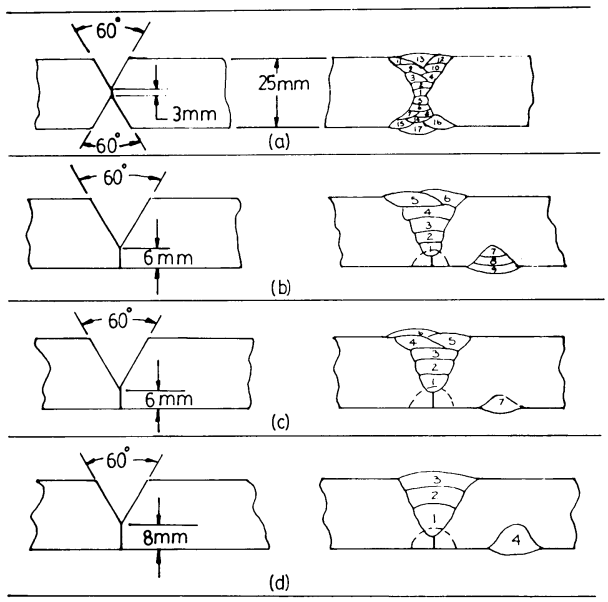

Fig. 1. Typical joint designs and pass sequences of experimental submerged arc welds: (a) 1.4 kJ/mm, (b) 2 kJ/mm, (c) 3 kJ/mm and (d) 4 kJ/mm.

notched at 1 mm from the fusion line shown schematically in Fig. 2. As indicated in 2.2, the simulated CGHAZ specimens were also notched through-thickness at the centre of the cycled region.

Charpy transition curves (based on the average of three samples) were obtained for weld metal and HAZ from tests conducted over the temperature range of −100 to 20°C.

Hardness measurements were made of the base material, CGHAZ and weld metal for all weldments and simulated samples. The data are expressed as Vickers hardness number for a 500 g load.

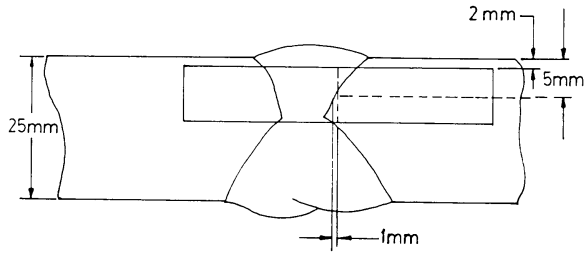

Fig. 2. Schematic diagram showing position of heat affected zone charpy test specimen, notched through thickness 1 mm from the fusion line.

2.4. *Microstructure evaluation*

The microstructural constituents of the weld metal and CGHAZ were determined by optical microscopy. Of particular interest was the identification of microstructure along the fracture path of the Charpy-V notch toughness specimens. Scanning electron microscopy was used on fractured Charpy specimen surfaces to determine the mode of fracture.

3. RESULTS

3.1. *Weld metal structure and mechanical properties*

The notch toughness properties of all welds from Series A and Series B weldments exceeded the notch toughness targets as shown in Fig. 3. For the Series A welds the notch toughness properties were mainly independent of heat input in the range of 1.4–4 kJ/mm. In the Series B welds the weld deposited at 4 kJ/mm was slightly lower in toughness in the lower temperature regime. In the upper shelf region of the Charpy transition curve the Series A welds were slightly higher in impact energy than the Series B welds.

The tensile properties listed in Table 3 indicated that all welds exceeded the required yield strength of 565 MPa. With

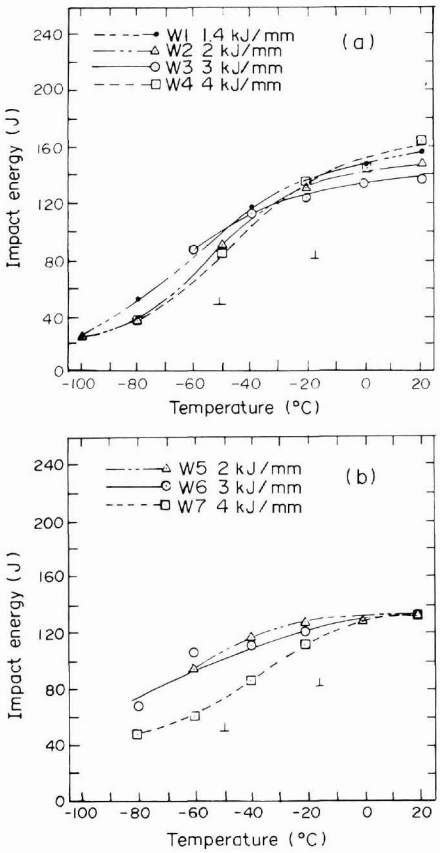

Fig. 3. Charpy transition curves for weld metals deposited with (a) Linde 95 and OP121TT (series A) and (b) LA100 and 880M wire/flux (series B) combinations. Notch toughness targets indicated by symbol ⊥.

Table 3. Tensile properties of submerged-arc weld metals

Weld No.	Yield strength (MPa)	Ultimate strength (MPa)	Elongation (%)	Reduction in area (%)
W1	689	779	27	70
W2	622	790	23	68
W3	632	835	21	65
W4	603	766	25	65
W5	626	935	21	63
W6	668	875	20	64
W7	600	822	21	65

Table 4. Microhardness results of HY80 weldments

Weld No.	Heat input (kJ/mm)	HAZ (DPH)	Weld metal (DPH)
W1	1.4	411	258
W2	2	409	230
W3	3	402	237
W4	4	364	231
W5	2	396	239
W6	3	397	238
W7	4	356	240

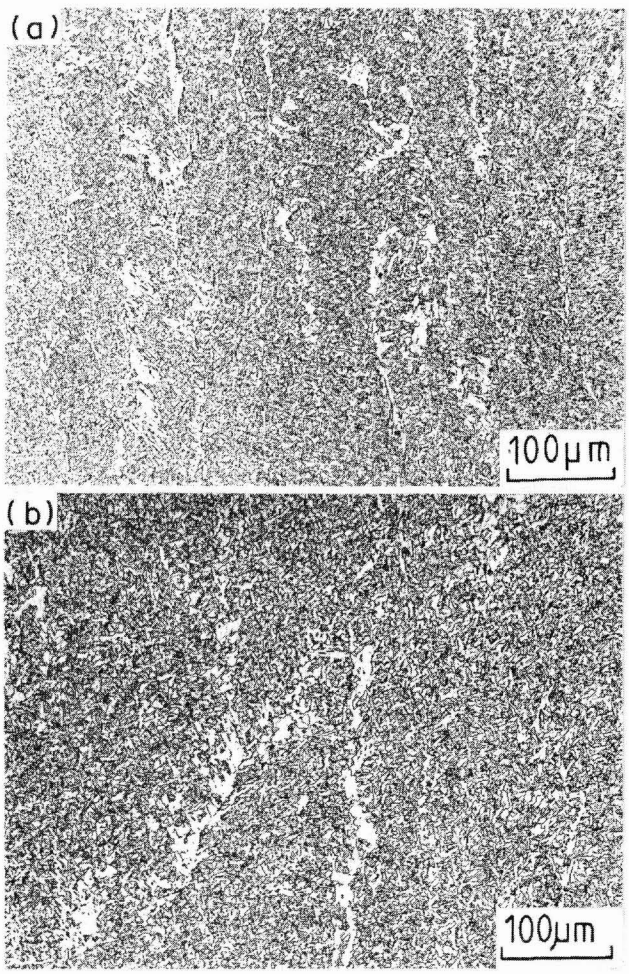

Fig. 4. As-deposited weld metal microstructures for SA welds (a) W2 and (b) W4.

the exception of weld W6 the yield strength decreased as the heat input was increased to 4 kJ/mm. Table 4 shows a similar trend with weld metal and HAZ microhardness values also decreasing.

The acceptable tensile and notch toughness properties found in the Series A and B weld metals can be attributed to a weld microstructure which contained acicular ferrite with a very low proportion of grain boundary ferrite and ferrite with second phase in both the as-deposited and reheated weld metal regions (Fig. 4). The only real difference between the as-deposited and reheated regions was that the tempering effect of subsequent passes caused some precipitation of carbides which decorated grain boundaries in the reheated region. These microstructural observations were found for both the low and high heat inputs. The sulfur and oxygen contents of Series A and B weld metals (Table 5) resulted in an inclusion content that produced completely ductile fracture and high Charpy shelf energies for test conducted at 20°C (Fig. 3). It should be noted that, although the oxygen level decreased with heat input, there was no significant change in Charpy shelf energy.

3.2. *HAZ mechanical properties*

The notch toughness properties of the weld specimens notched 1 mm from the fusion line are shown in Fig. 5 as a function of energy input. The notch toughness targets are

Table 5. Chemical compositions of submerged arc weld metals

Weld No.	Wt%														
	C	Mn	Si	P	S	Ni	Cr	Mo	Al	Cu	V	Nb	B	N	O
W1	0.060	1.30	0.405	0.010	0.005	1.88	0.37	0.350	0.02	0.055	<0.005	<0.005	—	0.0079	0.0379
W2	0.080	1.16	0.330	0.009	0.006	2.00	0.52	0.320	0.02	0.025	0.005	0.013	0.0003	0.0076	0.0327
W3	0.060	1.17	0.330	0.010	0.007	2.00	0.43	0.350	0.02	0.035	0.005	0.010	0.0004	0.0092	0.0310
W4	0.082	1.15	0.330	0.011	0.006	2.01	0.50	0.330	0.02	0.025	0.005	0.013	0.0003	0.0080	0.0261
W5	0.070	1.18	0.340	0.010	0.008	1.80	0.40	0.300	0.02	0.055	0.005	0.010	0.0003	0.0084	0.0312
W6	0.070	1.24	0.340	0.010	0.008	1.80	0.39	0.290	0.02	0.060	0.005	0.010	0.0003	0.0099	0.0275
W7	0.070	1.18	0.340	0.010	0.008	1.80	0.38	0.300	0.02	0.060	0.005	0.010	0.0004	0.0091	0.0268

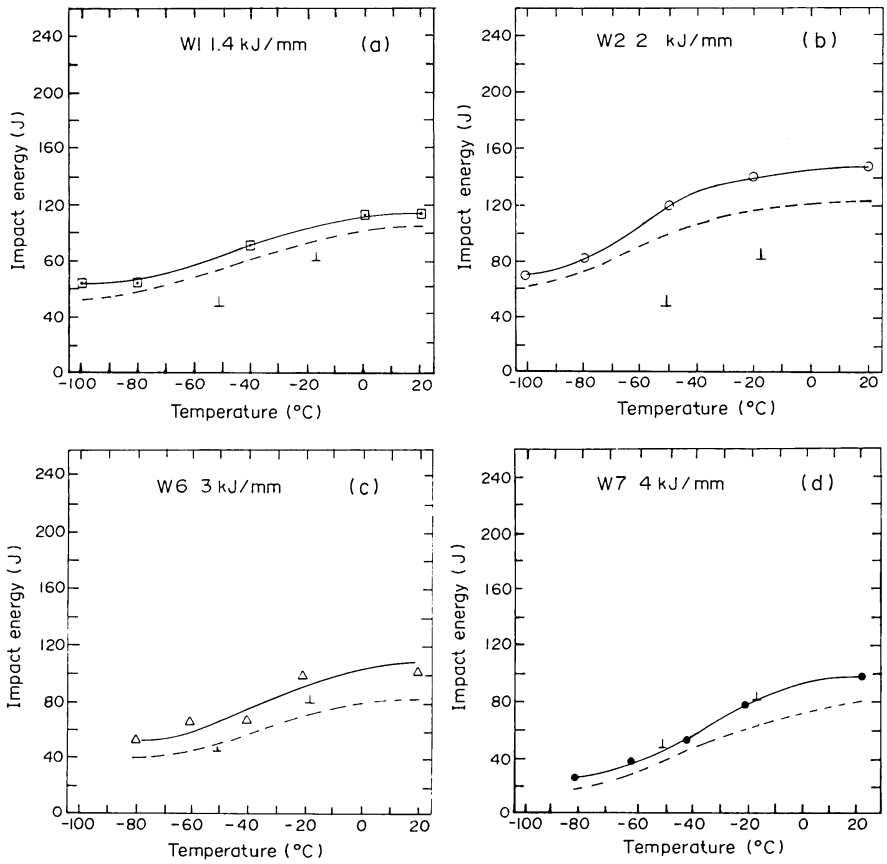

Fig. 5. Charpy transition curves for HY80 HAZ specimens notched 1 mm from the fusion line. Notch toughness targets indicated by symbol ⊥. Dashed lines represents lower scatter band: (a) 1.4 kJ/mm, (b) 2.0 kJ/mm, (c) 3.0 kJ/mm and (d) 4.0 kJ/mm.

indicated in each Figure. A significant decrease in notch toughness was observed only for energy inputs $\geqslant$ 3 kJ/mm. It should be noted, as shown in Fig. 2, that the root of the notch of the Charpy specimens resided not only in the CGHAZ but also in the weld metal, the finer grain regions of the HAZ and the base metal. This will be an important consideration in relating the notch toughness properties to microstructure.

As shown in Fig. 6, the notch toughness properties of the Gleeble simulated CGHAZ were poor, lying well below the specified toughness for both heat inputs in steel heats HT 1 and HT 2. The Charpy notch in this case resided totally in the CGHAZ structure.

3.3. *HAZ microstructure*

In order to explain the notch toughness properties of the real weld and Gleeble simulated HAZ's the microstructure along the fracture path must be evaluated.

The microstructure of the CGHAZ in the Gleeble simulated specimens is shown in Fig. 7. A totally martensitic structure was found for specimens cycled at both the 2 and 4 kJ/mm heat inputs. The CCT diagram for HY80 steel [10] indicated that a martensitic structure was expected for the cooling rates associated with these heat inputs. The hardness (Table 6) were of the order of 400 DPH for the Gleeble simulated samples. Another microstructural feature was the presence of

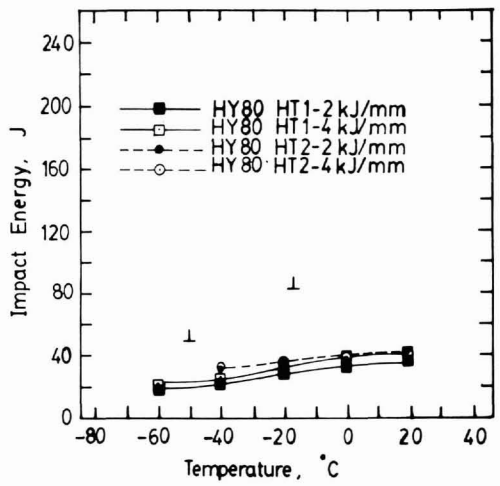

Fig. 6. Charpy transition curves of Gleeble simulated CG HAZ in HY80 steels. Notch toughness targets indicated by symbol ⊥.

Table 6. Microhardness results of Gleeble simulated HAZ

Sample	Heat input (kJ/mm)	Microhardness (DPH)
HY80 HT1	2	417
HY80 HT1	4	409
HY80 HT2	2	473
HY80 HT2	4	460

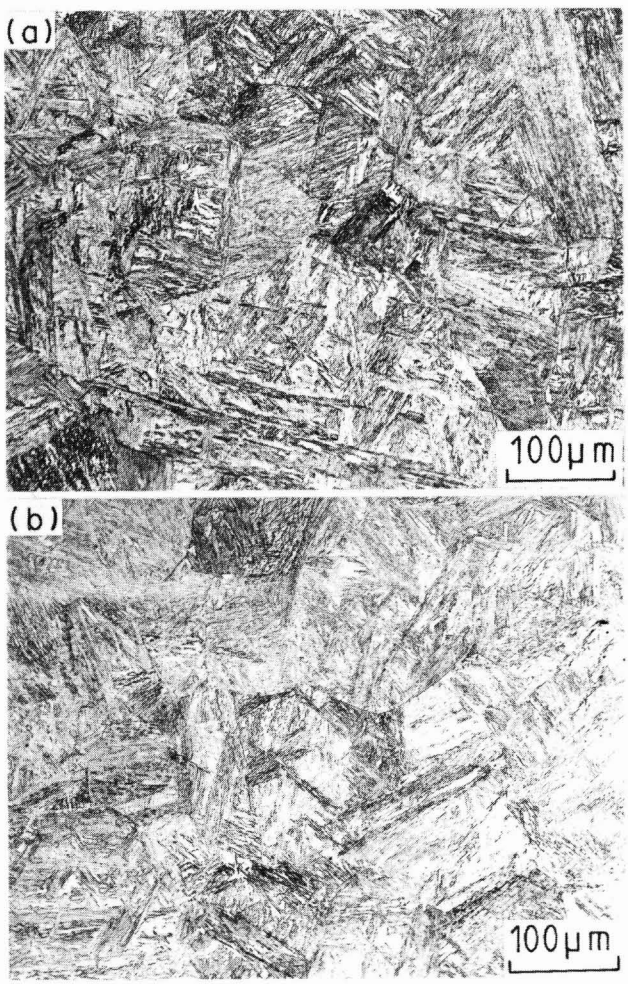

Fig. 7. CGHAZ microstructures of Gleeble simulated HY80-HT1 steel cycled to a peak temperature of 1350°C with cooling times of (a) $\Delta t_{8-5} = 11.5$ s (2 kJ/mm) and (b) $\Delta t_{8-5} = 45$ s (4 kJ/mm).

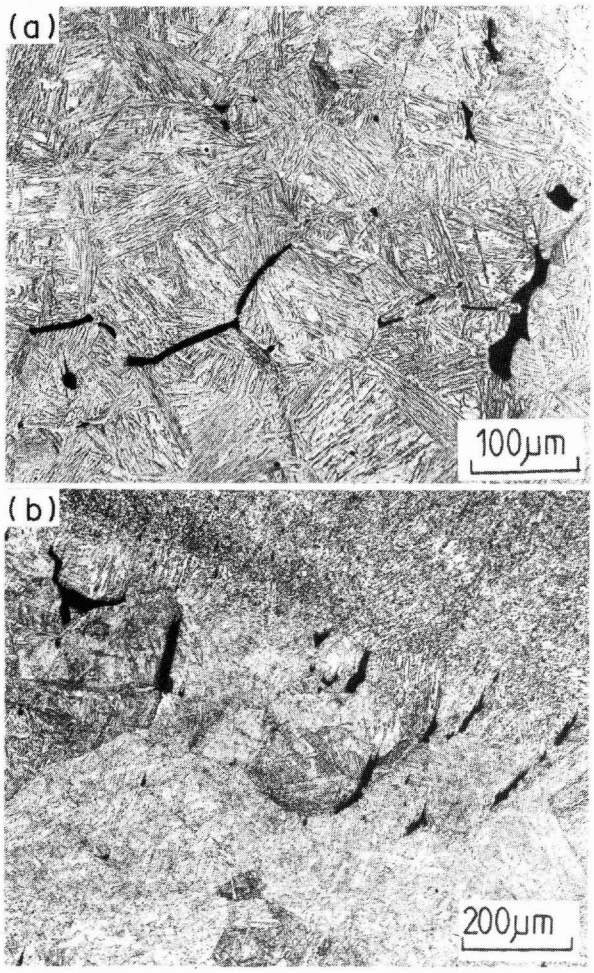

Fig. 8a. Microstructures of Gleeble simulated HY80-HT1 steel cycled to a peak temperature of 1440°C. Note microcracks along prior austenitic grain boundaries.

Fig. 8b. Microcracks in HY80-CGHAZ adjacent to the fusion line of the 4 kJ/mm submerged arc weld W4.

intercrystalline discontinuities. Although not readily observable at peak temperatures of 1350°C, they were found to be very prevalent in some samples cycled to higher peak temperatures as shown in Fig. 8a. The SEM examination of the fracture surfaces of the impact specimens provides evidence of the failure mode in the CGHAZ of the Gleeble simulated specimens. About 20–30% of the fracture surface exhibited an intercrystalline fracture mode shown typically in Fig. 9. This was more easily identified in specimens fractured at 20°C where the

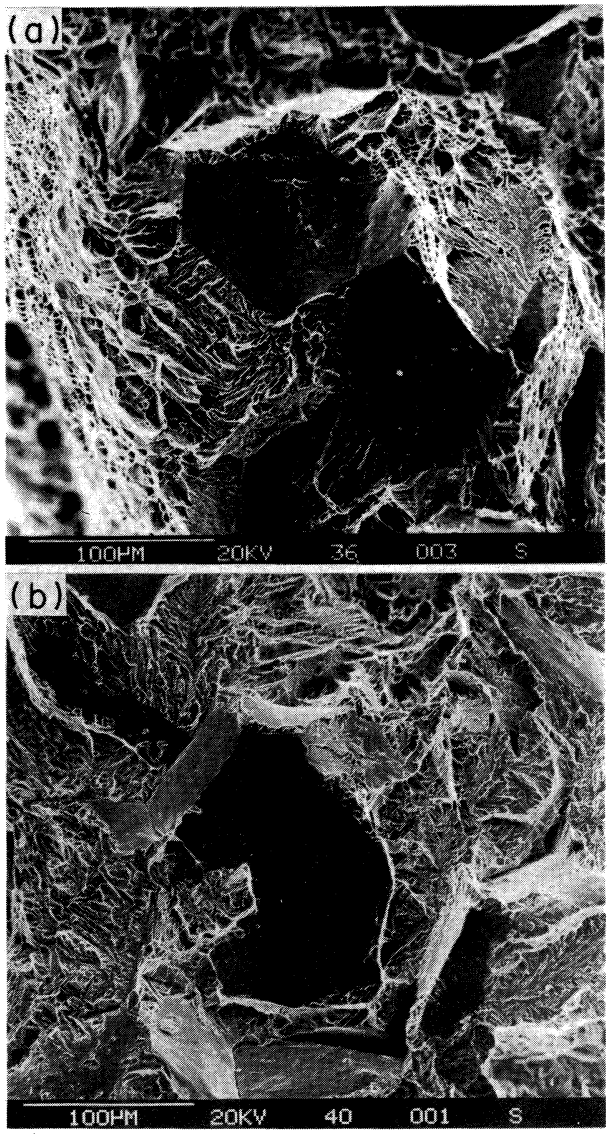

Fig. 9. Typical SEM fractographs of fractured Gleeble simulated Charpy specimens. (a) Charpy fracture surface showing ductile dimples and smooth intergranular facets. Impacted tested at 20°C. (b) Fracture surface of specimen tested at −40°C showing large intergranulara facets and quasi-cleavage fracture.

intercrystalline facets were surrounded by a mixture of ductile dimples and quasi-cleavage facets (Fig. 9a). It is likely that the tendency to intercrystalline failure in the CGHAZ was primarily responsible for the poor notch toughness properties of the CGHAZ simulated specimens in steel heats HT 1 and HT 2 at both heat inputs over the full test temperature range.

In the case of the real weld HAZ, it can be assumed, based upon the results of the Gleeble simulation experiments, that the CGHAZ is a local brittle region. For Chapry specimens notched 1 mm from the fusion line (Fig. 2), the fracture path was noted in sections cut perpendicular to the fracture surface immediately below the root of the notch. Typical fracture paths are shown schematically in Fig. 10. For welds deposited at 1.4 kJ/mm (Fig. 10a) the fracture path passed through the as-deposited weld metal, the CGHAZ, the fine HAZ and the base metal. Typically, the CGHAZ occupied about 10% of the

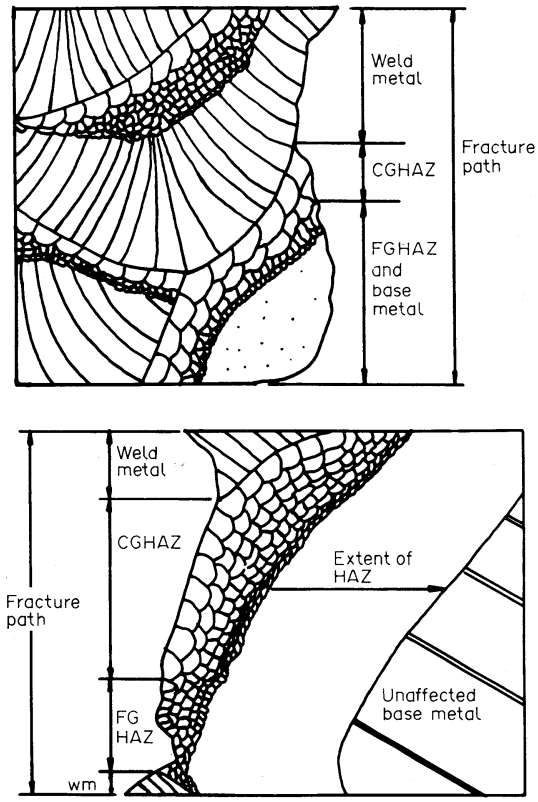

Fig. 10. Fracture paths in CVN specimen notched 1 mm from fusion line. (a) Schematic representation of fracture path in Charpy specimen sectioned perpendicular to the fracture surface below the root of the notch (magn. × 7.5). Fracture represents left hand portion of Charpy specimen designated in Fig. 2. Heat input 1.4 kJ/mm. (b) Fracture represents right hand portion of Charpy specimen designated in Fig. 2 (magn. × 7.5). Heat input 4 kJ/mm.

fracture path. At higher energy inputs, 4 kJ/mm in Fig. 10b, the CGHAZ was wider and the fracture path showed more tendency to follow along this region, i.e. the CGHAZ occupied more than 40% of the fracture path. The microstructural features of the CGHAZ in the real weld were similar to that observed in the Gleeble simulated specimens. At all heat inputs, the microstructure was composed of martensite (Fig. 11) with intergranular discontinuities shown typically in Fig. 8b. SEM studies of the fracture surface of the real weld HAZ Charpy specimens revealed that the fracture mode in the CGHAZ was primarily intercrystalline. Intercrystalline fracture facets similar to that found in the Gleeble simulated samples are shown in Fig. 12. Elongated stringers or "ferns" [5] that were identified as sulfides by EDAX, were observed (Fig. 12b) on most of the intercrystalline fracture facets. In relating the microstructural features of the CGHAZ to the notch toughness properties measured at 1 mm from the weld fusion line, it can be noted that the reduction in notch toughness properties for heat inputs $\geqslant$ 3 kJ/mm can be attributed to an increase in the amount of the embrittled CGHAZ taking part in the fracture process.

4. DISCUSSION

The notch toughness evaluation of high-strength HY80 weldments has shown that acceptable notch toughness properties can be achieved in submerged arc weld metals over a

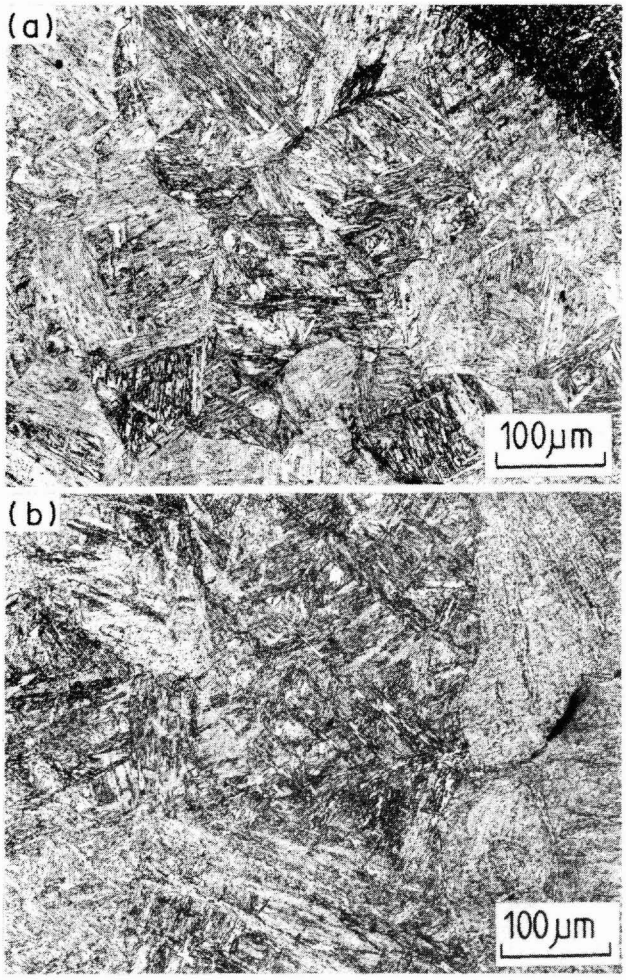

Fig. 11. Microstructures of the CGHAZ next to the fusion line in HY80 welds (a) Weld W2, (b) Weld W4.

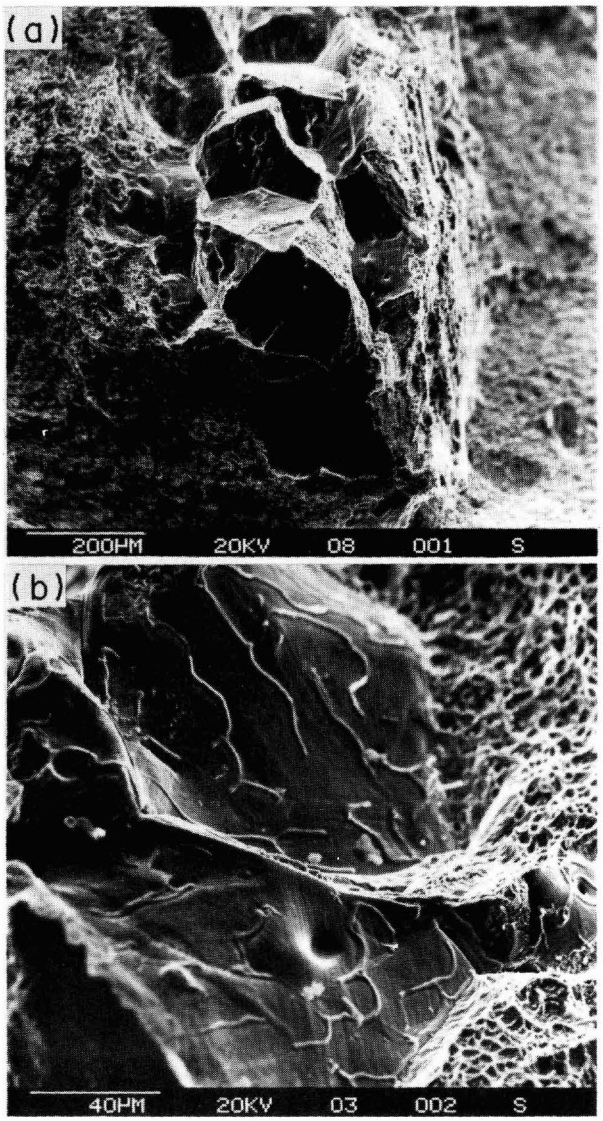

Fig. 12. SEM Fractographs of real weld CGHAZ Charpy impact specimens. (a) Fractograph showing isolated band of intergranular brittle fracture surrounded by ductile dimples in 4 kJ/mm Weld W7. (b) Intergranular failure showing sulfide "ferns" on facet surfaces.

range of heat inputs using commercially available welding consumables. On the other hand, the notch toughness measured at 1 mm from the fusion line was reduced at higher heat inputs because of embrittlement in the coarse grain heat-affected zone.

The high toughness of the weld metals was related primarily to the high proportion of fine grain acicular ferrite microstructure. The low carbon content of the weld metals, combined with hardenability contributions from the Mn, Ni, Cr and Mo additions (Table 5) resulted in this transformation product. Although no CCT diagrams of the weld metal compositions were available it was assumed that the ferrite region was shifted to longer times allowing the transformation of austenite to take place at sufficiently low temperatures resulting in a low proportion of coarse grain boundary ferrite and a high percentage of the acicular ferrite structure. This transformation to acicular ferrite took place over the range of cooling rates associated with heat inputs from 1.4 to 4 kJ/mm. The oxygen level of the weld metal can be considered as an additional factor in the transformation of acicular ferrite [2]. It has been shown that an oxygen level of 250–350 ppm results in oxide inclusions that can act as nucleation sites for acicular ferrite formation.

The Gleeble simulation studies have shown that the embrittlement produced in the CGHAZ can severely reduce the notch toughness of this region. This embrittlement was caused by liquation cracking. It has been well documented [4, 5] that liquation cracking occurs when the high peak temperature in the HAZ near the fusion line results in the melting of inclusions which then penetrate and weaken the austenitic grain boundaries. The tensile stresses generated in the welding cycle can produce discontinuities or microcracking along grain boundaries in the CGHAZ. The observations of sulfides on intercrystalline fracture facets were evidence of the resolidification of the liquated inclusions as sulfide films during cooling. These sulphides were more readily observed in the CGHAZ of real welds (Fig. 12) where slightly higher peak temperatures ($\sim 1400°C$) were achieved compared with the Gleeble simulation peak temperature of 1350°C. Liquation

cracking has been shown to increase with increasing carbon content and to decrease with increasing Mn/S ratio [11]. The results of Meitzner and Stout [11] have shown specifically in HY80 weldments that liquation cracking in the HAZ was extensive at a Mn/S ratio (22) and a carbon content (0.18%) which were similar to those found in the HY80 steels used in the present program.

From the results of the Gleeble simulation studies one can assume that the CGHAZ is a local brittle zone in the evaluation of the notch toughness near the fusion line of the HY80 weldments. It was shown that the CGHAZ region lowered the notch toughness in higher heat inputs welds, i.e. $\geqslant 3$ kJ/mm, when it occupied approx. 40% of the fracture path. These results agree with other recent studies of the effect of local brittle regions on weld fracture toughness. Kudoh and Pisarski [6] introduced local brittle zones into multi-pass C/Mn weld metals and showed that when 10% of the Charpy notch tip line sampled low toughness material the overall toughness was unaffected. However, the Charpy transition temperature of the weld was increased to that of the lowest toughness region when that region occupied more than 30% of the notch tip line.

In order to improve the toughness of the CGHAZ of HY80 steel, liquation cracking must be reduced. Increasing the Mn/S ratio may be the solution to the problem. The present base metal specification limits Mn addition to 0.40% maximum [12]. Thus in order to achieve a targeted Mn/S ratio of 100 in HY80 steel with carbon levels of the order of 0.18% the Mn can be increased to 0.40% but sulfur must be reduced to 0.004%.

5. CONCLUSIONS

(1) Notch toughness properties which exceeded the targeted Charpy energy levels of 81 J at -18°C and 47 J at -50°C were achieved in HY80 weld metals deposited by the SAW process using commercially available welding consumables.

(2) The high notch toughness properties in the weld metal were achieved by having a weld metal microstructure composed of a high (> 80%) proportion of acicular ferrite combined with a low inclusion content ($S + O \approx 0.04$%).

(3) Gleeble simulation studies of the CGHAZ in HY80 steel identified grain boundary embrittlement associated with liquation of sulfide inclusions. This embrittlement resulted in a reduction in notch toughness properties to well below targeted levels.

(4) The effect of the embrittled CGHAZ on the notch toughness measured near the fusion line in real welds in HY80 steel was to lower the notch toughness when the CGHAZ occupied approximately 40% of the fracture path in a Charpy impact test specimen. The drop in toughness occurred in welds deposited with heat inputs $\geqslant 3$ kJ/mm.

Acknowledgements—The authors wish to acknowledge the support of the Defence Research Establishment (Atlantic), and in particular Dr J. Matthews. They also wish to thank D. E. Dolan and D. P. Lusk for their assistance in performing experimental welding and radiographic inspection, respectively.

REFERENCES

1. R. W. Flax, R. E. Keith and M. D. Randall, ASTM STP494 (1971).
2. R. E. Dolby, *Metals Tech.* **10**, 349 (1983).
3. K. Masubichi and D. C. Martin, *Welding J.* **41**, 375-s (1962).
4. R. H. Phillips and M. F. Jordan, *Metals Tech.* **3**, 571 (1976).
5. R. H. Phillips and M. F. Jordan, *Metals Tech.* **4**, 396 (1977).
6. J. Kudoh and H. G. Pisarski, *Welding Inst. Res. Rep.* 294 (1986).
7. K. Satoh and M. Toyoda, *WRC Weld. Res. Abroad* **28**, 13 (1982).
8. Y. Mutoh, M. Toyoda, K. Satoh and S. Doi, *Trans. Am. Soc. mech. Engrs.* **106**, 16 (1984).
9. U.S. Dept of Defence, Military Specification MIL-STD-1688 (SH) (1981).
10. G. N. Emmanuel, D. E. Young and G. L. Spahr, *Metall. Engrs Ql* **1**, 82 (1961).
11. C. F. Meitzner and R. D. Stout, *Weld. J.* **45**, 393s (1966).
12. U.S. Dept of Defence, Military Specification MIL-S-162/16J(SH) (1981).